RSC Advances

Accepted Manuscript

This article can be cited before page numbers have been issued, to do this please use: H. Joshi, A. Sengupta, K. Gavvala and P. Hazra, *RSC Adv.*, 2013, DOI: 10.1039/C3RA42462F.

View Article Online
DOI: 10.1039/C3RA42462F

Unraveling the mode of binding of the anticancer drug, topotecan with dsDNA

Hrishikesh Joshi, Abhigyan Sengupta, Krishna Gavvala, and Partha Hazra*

Department of Chemistry, Mendeleev Block, Indian Institute of Science Education and Research (IISER), Pune 411008, Maharashtra, India.

* Corresponding author. E-mail: p.hazra@iiserpune.ac.in. Tel.: +91-20-2590-8077; Fax: +91-20-2589 9790.

View Article Online
DOI: 10.1039/C3RA42462F

Abstract

Binding interaction between antitumor drug and DNA is of burgeoning interest due to its upraising demand in medicinal science. In present work, we have tried to examine the mode of binding of topotecan (TPT) with DNA. TPT, an eminent anti-cancer drug from Camptothecin family, is found to interact with DNA Topoisomerase-I and inhibits DNA replication process. Steady state, time resolved fluorescence, circular dichroism and thermal melting studies have been utilized to explore the mode of binding of TPT with synthetic polynucleotides ($(dA\text{-}dT)_{15}$, $(dG\text{-}dC)_{15}$) and natural DNA (CT-DNA). The mode of binding of TPT with the DNA double helix has been substantiated to be principally groove binding. It is found even though the ground state cationic form (C) of the drug binds to dsDNA irrespective of DNA sequences, the emission mainly appears from Z^*, and it is attributed to the intermolecular excited state proton transfer (ESPT) reaction between drug and surroundings water molecules. However, in case of $(dA\text{-}dT)_{15}$, emission profile indicates the existence of small population of excited state cationic form (C^*) of the drug in the minor groove of DNA. The different photophysical behavior of TPT in case of $(dA\text{-}dT)_{15}$ compared to others is attributed to narrower and deeper minor groove of $(dA\text{-}dT)_{15}$ than the others. The exact molecular picture of binding interaction between drug and DNAs has been explored from molecular modeling studies.

Keywords: topotecan · DNA · spectroscopic methods · minor groove binding · molecular docking

View Article Online
DOI: 10.1039/C3RA42462F

Introduction

Chemotherapeutic agents share the spotlight over the decades due to their uprising demand in medicinal science. Although the anti-cancer activity of chemotherapeutic drugs is well known, the exact mode of action in many cases is still under debate. Therefore, chemotherapeutic drugs are burgeoning interest to the researchers.[1-4] Among many others, Topotecan (TPT), a penta-cyclic water soluble alkaloid member from Camptothecin family is the point of our interest due to its proven inhibitory activity against animal as well as human tumors. CPT was first isolated by Wall *et al*. in 1966 from a Chinese tree *Camptotheca acuminate.*[5] Water solubility is the main advantage for TPT compared to other drugs of Camptothecin family, and it mainly exists in two forms in water, namely, lactone form, responsible for TPT's anticancer activity, and carboxylate form, which does not show any anti-tumor action.[6,7] Note that, where most of the well known anti-cancer drugs are found to inhibit DNA Topoisomerase-II, TPT selectively interacts with Topoisomerase I (Topo-I) and inhibits DNA replication, and leads to necrosis or cell death [4, 8-10]. This overall process is believed to be governed by a ternary complex formation between DNA-TPT and Topo-I [11], though it was shown that TPT can solely interact with DNA in absence of Topo-I.[12]

More recently, Nunzio *et al.* reported elaborative pH dependent studies and solvent effect on the structural dynamics of TPT, and it was found that TPT exists in different protolytic forms depends on the pH as well as solvent.[13,14] It was observed that under physiological conditions (pH 7), the drug exists in equilibrium between the enol (E), cationic (C) and zwitterionic (Z) forms in the ground state (Scheme 1).[13,14] Interestingly, TPT exhibits a single fluorescence peak (~530 nm) in aqueous solution responsible for the emission from Z*, which is believed to be an outcome from excited-state proton transfer (ESPT) from TPT to water.[15] At physiological pH,

View Article Online
DOI: 10.1039/C3RA42462F

TPT hydrolyses to toxic carboxylate form,[16] and this appears to be a strong challenge for the researchers. Therefore, ongoing efforts have been invested to carry out active lactone form to the desired location. Results show that stability of lactone moiety could be improved by encapsulating the drug either in liposome[17,18] or in cyclodextrin[19], which might solve the problem of carriage. Next, the mode of interaction with DNA and its mechanism is also a prime point of interest, which can improve the therapeutic importance of TPT. The mode of interaction for lactone TPT and DNA devoid of Topo-I was determined by Yang *et al.* by HPLC followed by NMR techniques.[20] The results conclude that the lactone form predominantly exists in presence of dsDNA and binds to DNA through intercalation, though the relative shifts (~0.15-0.2 ppm) reported from NMR spectra does not impressively match with regular intercalation process.[21-23] Again the possibility of intercalation of lactone form of TPT is questioned when Streltsov *et al.* showed by linear dichroism study that angle of orientation for bound TPT (quinoline part) with DNA base pairs is found to be less than 54˚.[24] This value is clearly less than classical intercalator (62˚-76˚) and close to minor groove binders (< 55˚), which suggests TPT act as a minor groove binder.[24] Not only the mode of binding, the sequence specificity of TPT for DNA is also under strong debate. Yang *et al.* reported that lactone form of TPT is highly selective towards the poly(dG-dC) compared to poly(dA-dT) for intercalation.[20] Interestingly, Yao *et al*. reported that sequence specificity of TPT is toward dT of dsDNA instead of GC rich region,[12] which contradicts previous report. The ongoing quest about TPT's mode of binding along with sequence selectivity attracts our attention, and we have carried out thorough investigations to exterminate the contradictions engendered about TPT and DNA interaction. Absorption, steady state emission, circular dichroism (CD), and thermal melting studies have been employed to delve binding mode, specificity and affinity of TPT with DNA. The dynamics aspects of the

View Article Online
DOI: 10.1039/C3RA42462F

interactions are also highlighted through time-resolved fluorescence as well as rotational relaxation measurements.

TPT being an important anticancer drug, the detailed mechanism of interaction is helpful to enhance the therapeutic efficiency of the drug, as stronger binding to DNA backbone along with increased pose time in bound state enhances the therapeutic efficiency of drugs.[25,26] Moreover, specific binding of TPT to DNA makes it possible to use this drug as a fluorescence marker in histochemical studies to exclusively locate DNA or chromosome in cells.[27-29] TPT's sequence specific binding in DNA may further be useful to trace particular short sequence repeats, which have got great importance in DNA polymorphism.[30,31] We hope this new understanding will pave a way to divulge specific details about the interaction scenario of a renowned anti-carcinogen TPT with DNA, which may help in a better way in designing, targeting and tracing several cellular phenomena *in vitro* as well as in cells.

Experimental Section

(i) Materials, Methods and Instrumentation

Topotecan (High purity ≥ 99%), Calf Thymus DNA (CT-DNA) were purchased from Sigma Aldrich and used without any further purification. $(dA\text{-}dT)_{15}$ and $(dG\text{-}dC)_{15}$ were procured from Integrated DNA Technologies (IDT) and purified using SDS-PAGE gel purification technique. The concentrations of $(dA\text{-}dT)_{15}$ and $(dG\text{-}dC)_{15}$ were calculated by using cumulative molar extinction coefficient of all bases generated by SciTools of IDT website (332200 M^{-1} cm^{-1} and 251400 M^{-1} cm^{-1}, respectively). CT-DNA concentration is calculated using molar extinction coefficient 6600 M^{-1} cm^{-1} per base.[32] Phosphate buffer (PB) of pH 5.1 was used for all measurements and each of the constituents of buffer was also procured from Sigma Aldrich. The

View Article Online
DOI: 10.1039/C3RA42462F

working concentration of topotecan was calculated using molar extinction coefficient at 380 nm (ε_{380} = 20000 M^{-1} cm^{-1})[24] and kept at 20 μM for all the studies.

Measurements of solution pH were done by pH-1500 (Eutech Instruments, USA) and cross verified by silicon micro sensor pocket sized pH meter (ISFETCOM. Co. Ltd., Japan). Absorption spectra of free and DNA bound TPT were recorded in Evolution-300 UV-Visible spectrophotometer (Thermo Fisher Scientific, USA). Steady state fluorescence measurements were executed in Fluoromax 400 (Horiba Jobin Yvon, USA). Fluorescence lifetime and time resolved anisotropy measurements were performed using time-correlated single photon counting (TCSPC) set-up from IBH Horiba Jobin Yvon (USA), detailed description of which is mentioned elsewhere.[33-36] The lifetime and anisotropy data were collected by excitation at 375 nano LED (FWHM=90 ps) and analyzed using IBH DAS6 software. Quality of lifetime and anisotropy fits was judged on basis χ^2 values and from the visual inspection of the residuals. The value of $\chi^2 \approx 1$ was considered as best fit for the plots. Experimental error in our TCSPC measurements was ±5%.

Circular dichroism (CD) spectra were recorded on a J-815 CD (JASCO, USA). Each CD profile is an average of 3 scans of the same sample collected at a scan speed 100 nm/min, with a proper baseline correction of the blank buffer. During CD measurement, DNA concentration was kept fixed and the concentrations of TPT were increased steadily. Melting study was performed using Varian Cary 300 Bio UV-Vis Spectrophotometer. All the steady state and time-resolved experiments were performed at 300 K.

(ii) Molecular Docking

The crystal structure of $(dA\text{-}dT)_n$ [d(ATATATATAT)] obtained from RSCB protein Data Bank (PDB ID 3EY0[37]) was used for docking study. We didn't get a similar crystal structure of (dG-

View Article Online
DOI: 10.1039/C3RA42462F

dC)$_n$ sequence, and therefore, we have chosen a crystal structure [d(CCGCCGGCGG), PDB ID 1QC1[38]] of close resemblance to our sequence. 1DCV[39] [d(CCGCTAGCGG)] has been utilized for docking study in place of CT-DNA. The energy optimization of TPT conformer has been done using HF/6-31G level of Gaussian 98 suite and the resultant energy minimized geometry was saved in Autodock 4.2 compatible format. We have used Lamarckian Generic Algorithm to find out mode of binding of TPT with DNA in Autodock 4.2 software [40-42]. At the beginning of the study all water molecules was removed and Gasteiger charges were computed followed by addition of hydrogen as required by Lamarckian Generic Algorithm[41]. As the approximate location of binding was not known, we fixed a 120 × 120 × 120 grid box dimensions along x, y, and z axes with grid spacing 0.56 Å to cover all the atoms DNA, and a blind docking was performed to locate the possible position of the probe. TPT was docked in DNA with 150 GA population size and 100 GA runs. The lowest possible energy structure has been searched out using rank by energy presentation. After selecting the possible locations of TPT, the size of grid box was decreased to 60 × 60 × 60 in respective directions with a grid spacing 0.375 Å to generate most stable docked form through finite docking studies. The respective structure has been used for visualization through python molecular viewer. The final structure for presentation has been generated using chimera.[43]

Results and Discussion

1. Absorption Study

All the experiments of TPT are carried out at pH 5.1, as TPT exclusively exists in active lactone form at this pH (the pK_a of the carboxylic group is ~6.5) [14]. Although the drug can exist in different prototropic forms (Scheme 1), it mainly exists in cationic form in aqueous solution of pH 5.1, as the pK_a of dimethyl amino and 10-hydroxyl groups are 9.5 and 6.99, respectively.[14]

View Article Online
DOI: 10.1039/C3RA42462F

Notably, the DNA structure is not perturbed at this pH, as the pK_a for deprotonation of adenine, cytosine nucleobases are 3.5, 4.2.[44] TPT in phosphate buffer at pH 5.1 exhibits dual absorption bands at ~368 nm and at ~381 nm (Figure 1), which are attributed to the π-π* type absorption of the quinoline moiety. The very negligible absorbance at ~410 nm indicates ground state zwitterion (Z) form does not exist at this pH (Figure 1). With the gradual addition of $(dG\text{-}dC)_{15}$ and $(dA\text{-}dT)_{15}$, a decrease in absorption of both the peaks is observed (Figure 1). However, the peak at ~368 nm almost vanishes at maximum concentration of DNA (100 μM), whereas ~381 nm retains with a decreased absorption. Such changes in absorption spectral features of TPT clearly indicate the strong interaction between DNA and TPT. Considering favorable electrostatic stabilization between the cationic form of drug and negatively charged phosphate backbone of DNA, we believe preferably cationic form of the drug interacts with DNA compared to other forms (enol or zwitterionc form) of the drug. Similar kind of observation has been reported in case of sanguinarine where also the cationic form of the drug strongly interacts with DNA compared to enol form.[45] Existence of an isosbestic point at ~387 nm indicates the presence of equilibrium between free drug and DNA-bound drug. To check the interaction behavior of the drug with wild DNA, we have also probed interaction behavior between TPT and CT-DNA, and it shows close resemblance with the synthetic polynucleotide absorption changes (see Figure S1a in SI). The association constants for TPT-DNA (insets of Figure 1) interaction have been calculated from half reciprocal plot [46] using the changes observed at 381 nm, which are found to be 1.35×10^4 (±10%) M^{-1} , 1.23×10^5 (±10%) M^{-1} and 4.8×10^3 (±10%) M^{-1} for $(dG\text{-}dC)_{15}$, $(dA\text{-}dT)_{15}$ and CT-DNA, respectively. The association constants along with the free energy changes (-5.71 kcal/mol, -7.03 kcal/mol and -5.08 kcal/mol for $(dG\text{-}dC)_{15}$, $(dA\text{-}dT)_{15}$ and

View Article Online
DOI: 10.1039/C3RA42462F

CT-DNA, respectively) infers that the ground state binding between drug and DNA is thermodynamically favorable process.

2. Fluorescence Study

The DNA induced modification to the steady-state emission profile of the drug is depicted in Figure 2. The emission profile of TPT in aqueous buffer medium at pH 5.1 is characterized by a single unstructured band at 530 nm upon excitation at 380 nm. It is already established that the excited state zwitterion (Z^*) form of TPT is the main emitting species in water (pH 6.25), while the fluorescence from C^* is not detectable in water (pH 6.25).[13] Therefore, the emission peak at 530 nm of TPT in aqueous solution is originating from Z^* form of TPT. It's interesting to notice that although the cationic form of TPT (C-TPT) is major ground state species at this pH, the outcome fluorescence is from Z^*. This observation is attributed to the excited state proton transfer (ESPT) reaction from 10-hydroxyl group of C-TPT to water, and leads to the formation of Z^* in the excited state.[15] Similar kind of ESPT process was already reported in case of 10-hydroxy camptothecin by Solntsev *et al*.[47] As displayed in Figure 2a, on gradual addition of $(dG\text{-}dC)_{15}$, emission intensity at 530 nm progressively decreases, and it exhibits almost 50% quenching at maximum concentration of DNA (~100 μM) without any shift in emission position. On the other hand, addition of $(dA\text{-}dT)_{15}$ produces relatively lower intensity quenching (~35%) with a slight blue shift of emission position (~5 nm). Astonishingly, in case of $(dA\text{-}dT)_{15}$ a peeping peak appeared at ~420 nm, and at maximum DNA concentration (~100 μM) it appears as a prominent peak (Figure 2b). Decreasing intensity at 530 nm for both the synthetic dsDNA infers the relative lowering of Z^* population of TPT through the interactions with the above mentioned DNA. The appearance of 420 nm emission peak (Figure 2b) infers that some population of TPT remains in C^* instead of converting to Z^* in the excited state after binding to

View Article Online
DOI: 10.1039/C3RA42462F

$(dA\text{-}dT)_{15}$. Interesting to note that the population of C^* is not present in case of $(dG\text{-}dC)_{15}$ (Figure 2a) and CT-DNA (Figure S1b in SI), as 420 nm peak does not appear in those systems. Although the exact reason for such selective interaction is difficult to conclude at this point, however, after confirmation of binding modes of TPT, we hope that we will be able to predict more precisely, why $(dA\text{-}dT)_{15}$ selectively preserves excited state cationic (C^*) form of TPT.

After exploring the trends in emission, we have tried to elucidate the possible mechanism of quenching. Usually, there are two distinct possibilities of quenching, namely, photo-induced electron transfer (PET) or photo-induced energy transfer. The possibility of energy transfer can easily be ruled out as it needs overlap between emissions of donor (Z^* TPT) and absorption of acceptor (nucleobases), which is not possible in the present case. Therefore, the most plausible mechanism for fluorescence quenching is PET between TPT and nucleobases, as it is already reported that PET between drug and nucleobases leads to fluorescence quenching.[48-51] Note that, guanine is a better electron donor among all nucleobases[49], and hence, poly(dG-dC) sequence exhibits more quenching effect compared to poly(dA-dT). When nucleobase(s) of dsDNA participates in quenching it demands a close proximity to the drug. There are three distinct possibilities for a drug to interact with a dsDNA in a close proximity, namely intercalation, groove binding and electrostatic interaction. Although the first two processes can lead to quenching of fluorescence intensity, electrostatic interaction alone cannot lead to fluorescence quenching in such an extent. The changes in emission intensity have been utilized to calculate the Stern-Volmer (S-V) quenching constant. S-V plot shows a straight line fit for $(dG\text{-}dC)_{15}$ ($K_{SV} = 9.6\times10^3\ M^{-1}$), whereas a curved plot towards X-axis is obtained for $(dA\text{-}dT)_{15}$ sequence (Figure S2). A straight line S-V plot is strongly indicative towards the fact that TPT molecules are bound to $(dG\text{-}dC)_{15}$ DNA in a single mechanistic manner. Whereas curvature towards x-axis in S-V plot

View Article Online
DOI: 10.1039/C3RA42462F

is suggestive towards the concomitant existence of two different distributions of TPT molecules in presence of $(dA\text{-}dT)_{15}$. The quenching results are corroborative with our fluorescence spectral features, where it has been observed that only zwitterion form (Z^*) of TPT is the sole emitting species in case of $(dG\text{-}dC)_{15}$, but in presence of $(dA\text{-}dT)_{15}$ both of C^* and Z^* are the emitting species, although the latter species are in majority.

Binding constant is calculated for the quantitative representation of drug-DNA binding affinity using the following equation[52-54],

$$\log[(F_0\text{-}F)/F] = \log K + n \log[Q] \qquad (1)$$

where, F_0 and F are the fluorescence intensities of the drug (at 530 nm) in absence and presence of polynucleotides, respectively. A graph of $\log[(F_0\text{-}F)/F]$ versus $\log[Q]$ yields K and n (see insets in Figure 2), which represent binding constant and number of binding sites, respectively. A linear plot for $(dG\text{-}dC)_{15}$ system generates K and n values 3.3×10^3 (±10%) M^{-1} and 0.9, respectively. For $(dA\text{-}dT)_{15}$, we have obtained a curved plot. Hence, binding constant is calculated using experimental points up to which the plot is linear, and is calculated to be 0.8×10^3 (±10%) M^{-1}. The binding constant for TPT binding with CT-DNA is found to be 0.54×10^3 (±10%) M^{-1}. Corresponding free energy changes are -4.83 kcal/mol, -4.0 kcal/mol and -3.77 kcal/mol for $(dG\text{-}dC)_{15}$, $(dA\text{-}dT)_{15}$ and CT-DNA, respectively. The binding affinity of the drug obtained from fluorescence study is slightly less than that of absorption study presumably because in emission we have monitored the intensity of zwitterionic form, which probably has less binding affinity compared to cationic form of the drug in the ground state. We have also done similar experiments with $(dG\text{-}dC)_7$ and found that the binding constant with TPT is 1.03×10^3 (±10%) M^{-1}(Figure S3 in SI) which is closely resemble to the association constant of TPT

View Article Online
DOI: 10.1039/C3RA42462F

with $(dG\text{-}dC)_{15}$. These findings clearly demonstrate that the length of flanking bases has negligible role on binding affinity of TPT with dsDNA.

Up to this point, we are certain that drug is interacting with dsDNA, however, we cannot precisely predict the mode of binding. To elucidate the proper mechanism of interaction between drug and dsDNA, we have carried out several studies, like, intercalator displacement assay, KI titration and salt concentration dependent fluorescence, circular dichroism, time-resolved experiments and molecular modeling study, which are discussed hereunder.

3. Ethidium bromide (EtBr) displacement assay and KI titration

Among different modes of interactions (namely, intercalation, groove binding, and electrostatic), we first consider the possibility of intercalation through EtBr displacement assay experiment (Figure S4). It is already evident from fluorescence experiments that TPT emits at ~530 nm in presence of $(dG\text{-}dC)_{15}$, whereas a dual emission at 530 nm and 421 nm appears in case of $(dA\text{-}dT)_{15}$. With increasing EtBr concentration (up to 40 μM) in TPT-DNA systems, we observe a dominant emission peak at ~600 nm, which is the signature peak of EtBr intercalating in DNA.[55,56] Interestingly, no emission enhancement is observed at 530 nm in presence of EtBr. If TPT acts as an intercalator, then one would expect an instant replacement of TPT molecule from DNA by one of the most efficient intercalator EtBr, and as an outcome the emission of TPT would retract back to its initial intensity as obtained in aqueous medium. As no such changes in TPT spectra have been observed through EtBr displacement assay, one can definitely conclude that TPT is not binding to either $(dG\text{-}dC)_{15}$ or $(dA\text{-}dT)_{15}$ through intercalative binding mode.

Monitoring the quenching of fluorescence of free TPT and DNA-bound TPT paves also a way for simple but efficient technique for exploring mode of binding of the drug with DNA. I^- being an excellent quencher can be used to clarify the type of interaction between drug and

View Article Online
DOI: 10.1039/C3RA42462F

DNA. I^- can quench either electrostatically bound or groove bound drugs as these positions are fully and partially accessible by the quencher, whereas, for intercalated drugs hardly any quenching can be observed.[52, 54] When KI is employed as an external quencher, we found that its quenching efficiency toward TPT is reduced in presence of DNA compared to TPT-KI interaction in absence of DNA (Figure S5). The observation of quenching effect of TPT even in presence of either $(dA\text{-}dT)_{15}$ or $(dG\text{-}dC)_{15}$ supports electrostatic or groove binding mode of binding of TPT into DNA double strands, since electrostatic or groove binding leads to ample exposure of fluorophore to the bulk aqueous buffer phase. The quenching effect is greater in case of $(dG\text{-}dC)_{15}$ compared to $(dA\text{-}dT)_{15}$, and it is attributed to wider minor groove of $(dG\text{-}dC)_{15}$ than the $(dA\text{-}dT)_{15}$[57,58]. TPT bound to wider groove of $(dG\text{-}dC)_{15}$ can relatively be more exposed to KI compared to $(dA\text{-}dT)_{15}$, where the drug is located in narrow minor groove. In a nutshell, the fluorescence studies clearly infer that TPT doesn't involve in intercalative mode of binding to the dsDNA. This conclusion is further confirmed by thermal melting study of DNA in presence of TPT (Figure S6 in SI). DNA intercalation being the strongest mode of interaction offers large change in melting temperature.[22,59] However, we observed no prominent change in melting temperature either for $(dA\text{-}dT)_{15}$ or $(dG\text{-}dC)_{15}$. Therefore, thermal melting study corroborates well our conjecture from fluorescence studies, where we have also found that TPT does not interact with dsDNA through intercalative mode of binding.

4. Salt concentration dependence assay

Salt concentration dependent assays are good tool to verify the role of electrostatic interactions between drug and DNA. To elucidate the type of interaction between TPT and DNA, we have carried out the same experiment of TPT-DNA titration in presence of high NaCl concentration (Figure S7). Interestingly, when the TPT was titrated by DNA in PBS having NaCl

View Article Online
DOI: 10.1039/C3RA42462F

concentration of 100 mM, we have observed that the quenching effect of TPT is less compared to the changes observed in non NaCl buffer medium (PB). This observation suggests that electrostatic interaction also plays a role in the TPT-DNA interaction. Here it is pertinent to mention that NaCl (a source of Na^+ ion) can effectively screen the negative charge of phosphate backbone of DNA and weakens the possible electrostatic attraction between positively charged drug and DNA. Moreover, Na^+ and other monovalent alkali metals are very well known for their groove binding and groove narrowing effects.[60-62] Eventually, the minor groove becomes narrower when Na^+ binds to outer edge of groove having a direct contact with the phosphates.[60-62] The lower extent of change for $(dA\text{-}dT)_{15}$ is likely to be due to narrower groove size (3-4 Å) of poly(dA-dT) compared to poly(dG-dC) groove (5-7 Å).[57,58,60] In presence of 100 mM NaCl, the groove width of poly(dA-dT) becomes narrower. Therefore, it is very likely that molecule cannot fully access the minor groove in this condition, and as a result quenching effect is less in presence of NaCl. Peak of cationic (C^*) form of TPT at 420 nm, which becomes visible after addition of $(dA\text{-}dT)_{15}$, could not be observed in phosphate buffer containing 100 mM NaCl (Figure S7b). This may be attributed to the fact that the drug molecule cannot fully access the minor groove at high salt concentration (as Na^+ ion reduces the groove size). Therefore, the drug is more exposed in water, and as a result cationic form (C) of TPT cannot exist in this exposed condition, as it subsequently converts to Z^* form of drug in aqueous environment. In case of wild DNA, almost similar effect is observed in presence of 100 mM NaCl.

5. Circular dichroism

Circular dichroism (CD) is very sensitive technique for elucidating the modification of secondary structure of biopolymers as a result of interaction with small molecules.[60,63-65] Therefore, we have exploited CD technique in order to confirm the probable mode of binding of

View Article Online
DOI: 10.1039/C3RA42462F

TPT with $(dA\text{-}dT)_{15}$, $(dG\text{-}dC)_{15}$, and wild CT-DNA using CD spectroscopy (Figure 3). In this study polynucleotide concentration is kept constant throughout the measurements and changes of CD spectra have been monitored with increasing concentrations of drug. CD spectrum of both the synthetic DNA shows a positive peak at ~275 nm, and a negative peak at 245-250 nm region which is signature of the right handed B-form[63,64] (Figure 3). These bands are originated by stacking interactions between the bases and the helical structure of the polynucleotide, respectively.[63-65] With the progressive addition of TPT, intensity of positive peak of both the DNA is found to be almost unperturbed and no induced CD is observed in the visible region. The unaffected bases stacking interaction and the absence of induced CD indicates that ~~the~~ intercalation is not the binding mode of TPT into the DNA helix, as intercalation leads to disrupt base stacking interaction significantly.[66] On the other hand, the reduced helicity of both the DNA (reflected by the decrease of ellipticity at around ~245-250 nm region, Figure 3) dictates that TPT interacts with dsDNA through groove binding mode, as it is known that groove bind can lead to the perturbation of ellipticity of DNA helix.[51] The similar observations are also found for wild CT-DNA (Figure S8 in SI). Therefore, CD results are well supportive with fluorescence and thermal melting results, where we have also observed that TPT interacts with DNA mainly through groove binding mode, although previous section we have found that electrostatic interaction also has slight role in the interaction process between TPT and DNA.

6. Time Resolved Study

6a. Lifetime Measurements

To get clear insight about the drug-DNA interaction, the time-resolved decays of TPT have been recorded in absence and in presence of various concentration of DNA exciting at 375 nm. The decays are shown in Figure S9 and results are summarized in Table 1. It is clear from

View Article Online
DOI: 10.1039/C3RA42462F

the fitting results that the drug exhibits bi-exponential decay feature at pH 5.1. The long and major component (5.79 ns, 93%) reflects the lifetime of Z^* form of TPT. However, the origin of the fast component of 0.79 ns, which has almost 7% contribution to the decay profile, is not clear to us. Notably, we have already mentioned that although we are selectively exciting the C form of drug, Z^* becomes major emitting species (λ_{em} = 530 nm) due to ESPT process. We believe that a small population of C^* is also contributing to the decay profile collected at 530 nm, due to the existence of protolytic equilibrium between C^* and Z^*. The data compiled in Table 1 reveals that the drug lifetime is almost unperturbed in case of $(dG\text{-}dC)_{15}$, even at highest DNA concentration. However, we have observed quenching effect of almost 60% in steady state emission profiles for $(dG\text{-}dC)_{15}$ sequence. Therefore, it is logical to conclude that TPT forms a ground state dark complex, when it binds to the minor groove of DNA, and this dark complex does not emit in the excited state. This conclusion remains same even for CT-DNA, as we did not notice any change in lifetime for CT-DNA and TPT interaction.

In case of $(dA\text{-}dT)_{15}$, the lifetime of short component progressively increases with the gradual addition of polynucleotide concentration (Table 1, Figure S9b in SI). At highest DNA concentration, the lifetime of short component is hiked to 2.3 ns together with increased relative contribution of 26%. As short component is already assigned to the cationic form of TPT, the increased lifetime along with the hiked relative contribution of short component infers that cationic form of TPT is getting stabilized in presence of DNA due to electrostatic interaction between the negatively charged phosphate backbone and the positive charge of the drug. The increased lifetime of long component, which is assigned to the lifetime of Z^* form of TPT, is attributed to stability gained by Z^* form of TPT when it binds to the minor groove of DNA. The decreased relative contribution of Z^* form of TPT is due to the slightly shifting of equilibrium

View Article Online
DOI: 10.1039/C3RA42462F

between Z^* and C^* towards the latter side. In case of $(dA\text{-}dT)_{15}$, we have also collected lifetime of cationic form (C^*) of TPT at 420 nm (Table 1b), as this peak appears in the emission profile of above mentioned synthetic DNA. It is clear from the analysis that the average lifetime of C^* form of TPT increases from 300 ps to 450 ps, inferring stability gained by the C^* form of TPT in presence of $(dA\text{-}dT)_{15}$. This corroborates well with the steady state observation where we have observed prominent enhancement of 420 nm emission peak in presence of $(dA\text{-}dT)_{15}$. In a nutshell the lifetime results infer that $(dA\text{-}dT)_{15}$ offers a distributed binding of different forms of TPT, whereas $(dG\text{-}dC)_{15}$ binds specifically one form of the drug. The molecular picture of the interaction between different forms of drug and dsDNA will be clear from molecular modeling study discussed in the later part of the manuscript.

6b. Anisotropy Measurements

Time resolved anisotropy offers a vivid glance about the system induced restrictions over the tumbling motion of emitting species at excited state.[67] The anisotropy decays of TPT in buffer and in presence of DNA are shown in (Figure 4). The rotational relaxation of TPT in buffer solution collected at 530 nm exhibits single exponential decay with a rotational diffusion time of 220 ps. Upon addition of $(dA\text{-}dT)_{15}$, the rotational motion of TPT is retarded manifold. At maximum $(dA\text{-}dT)_{15}$ concentration, TPT shows a dominant 4.3 ns component, which may be attributed to DNA bound TPT (Figure 4). This significant alteration in rotational time of the drug is only possible when the drug resides in a highly restricted milieu. These results are in accordance with steady state and time resolved lifetime results, where we have inferred that Z^* form of TPT undergoes groove binding interaction with $(dA\text{-}dT)_{15}$. Other protolytic form of TPT, namely C^* form, which is generated in presence of $(dA\text{-}dT)_{15}$, also exhibits restriction in rotational motion (Table 2), as it also binds in the minor groove region of $(dA\text{-}dT)_{15}$. No such

View Article Online
DOI: 10.1039/C3RA42462F

changes have been observed in case of $(dG\text{-}dC)_{15}$, as it is already evident from steady state and time resolved studies that TPT forms dark complex when it binds to $(dG\text{-}dC)_{15}$. For CT-DNA, TPT also does not exhibit any change of rotational motion likewise $(dG\text{-}dC)_{15}$. The anisotropy results for $(dG\text{-}dC)_{15}$ and CT-DNA substantiate well with the steady state and time resolved lifetime results. Therefore, it is logical to conclude from above observation that in wild variety of DNA, TPT prefers to bind GC rich region rather than AT rich region.

The change in rotational diffusion time determined for free and trapped TPT has been exploited to evaluate hydrodynamic radius of the free and DNA bound drug using the following Stokes-Einstein relationship,[68]

$$\tau_r = \frac{1}{6D_r} = \frac{\eta V}{kT} \qquad (2)$$

where, D_r, η, V and T are the rotational diffusion coefficient, viscosity of the medium, hydrodynamic molecular volume of the complex and the temperature, respectively. The hydrodynamic diameter calculated form anisotropy data are found to be ~12 Å for free drug and ~33.5 Å for TPT bound to $(dA\text{-}dT)_{15}$ (100 μM). Almost ~20 Å increase in hydrodynamic diameter of the drug-DNA complex is conclusive about groove binding interactions of TPT. As TPT form dark complexes with $(dG\text{-}dC)_{15}$ and CT-DNA, we are not able to calculate the change in hydrodynamic radius when TPT binds to either of the above mentioned DNA.

7. Molecular modeling

Though crystal structure of the drug-DNA complex can provide the detail insight of the interaction, binding location and orientation of drug molecule can be qualitatively predicted through the docking studies. For docking studies, we have used cationic (C) form of topotecan, which is speculated to be interacting with dsDNA from our experimental results. Zwitterion form

View Article Online
DOI: 10.1039/C3RA42462F

(Z) of TPT is considered for docking study, as it is formed in excited state. The crystal structure of both poly(dA-dT) and poly(dG-dC) clearly indicates that minor groove size of the former is narrower and deeper than the latter, which is consistent with the literature reports.[57,58] According to docking studies, C-TPT binds in DNA minor groove of both the synthetic polynucleotides with variable orientation due to cumulative effect of hydrogen bonding, electrostatic attraction and Vander Waals force. Most stable structures on the basis of binding energy are depicted in Figure 5. In case of GC-duplex, C-TPT binds with binding energy -8.09 kcal/mol (Figure 5a). For C-TPT almost 100 docking structures with very small energy difference have been found. However, most of the cases TPT orientation in GC-minor groove is in such a way that its 10-hydroxy and 9-dimethyl amino methylene groups are projecting outward from groove, and therefore, it can access water environment, which is essential for the excited state conversion to zwitterionic form (Z^*) due to ESPT process. Interestingly, in case of poly(dA-dT) two types of orientations of DNA bound C-TPT are observed in the docking cluster with small difference in binding energy. Among the two different orientations, the -OH group of TPT projected inside the groove (Figure 5b) in one orientation (-11.67 kcal/mol); whereas in other orientation (-11.42 kcal/mol), the -OH group is away from groove (Figure 5c). In first case -OH group of TPT cannot access the water, and as a result water assisted ESPT process, which leads to C to Z^* conversion, does not take place. On the other hand, in the second orientation, -OH group away from the groove can access water, hence, C to Z^* conversion takes place. Therefore, in case of poly(dA-dT) emission peak appeared at 420 nm along with 530 nm, although the intensity in former case significantly lower than that of latter. This may be one of the reason for observing emission from both the C^* and Z^* forms of TPT in case of poly(dA-dT), whereas for poly(dG-dC) sole emission from Z^* is observed. Another plausible reason for not detecting C^* emission for

View Article Online
DOI: 10.1039/C3RA42462F

poly(dG-dC) is the larger minor groove width of poly(dG-dC) compared to poly(dA-dT). Due to larger minor groove width, water accessibility to the minor groove of poly(dG-dC) is quite higher than the minor groove of poly(dA-dT). Natural DNA (1DCV[39]) bound TPT (Figure S10) also exhibits similar binding orientations likewise poly(dG-dC), and therefore, exhibits emission only at 530 nm as that of poly(dG-dC).

Conclusion

The present work deals with the age old quest of TPT's mode of binding and sequence specificity to DNA. TPT in pH 5.1 has been studied with various synthetic dsDNA ($(dG\text{-}dC)_{15}$, $(dA\text{-}dT)_{15}$) as well as natural DNA (Calf thymus DNA) to find the exact mode and mechanism of binding. From EtBr displacement assay and thermal melting experiments, the possibility of intercalation of TPT lactone in dsDNA has been ruled out. However, KI titration and circular dichroism experiments confirm that TPT interacts with dsDNA through minor groove binding mode, although salt concentration experiment indicates that electrostatic interaction also takes part some role in this binding process. Interestingly, it has been found that irrespective of DNA sequence, TPT emission is getting quenched when it binds to DNA, and it has been attributed to photo-induced electron transfer between nucleobases and drug. Moreover, TPT emission mainly comes from the Z^* form of the drug irrespective of DNA sequences, and it has been ascribed to excited state ESPT process by which excited cation (C^*) converts to Z^* form. Astonishingly, slight population of excited state cationic form (C^*) of TPT is observed in case of $(dA\text{-}dT)_{15}$ and exhibits an emission peak at around ~420 nm, although the emission from Z^* dominates over the C^* emission. The observed different photophysical behavior of the drug in different DNA sequence is attributed to the narrower and deeper minor groove width of $(dA\text{-}dT)_{15}$ compared to $(dG\text{-}dC)_{15}$ and CT-DNA. The groove width of $(dA\text{-}dT)_{15}$ offers the tighter binding of the drug,

View Article Online
DOI: 10.1039/C3RA42462F

and this is supported by time-resolved anisotropy measurement, where we found the drug tumbling motion drastically retarded when it binds to the $(dA\text{-}dT)_{15}$ irrespective of the form(s) of the drug binds to DNA. Finally, molecular modeling study has been performed to get insight into the molecular picture of the interaction between drug and dsDNA. In case of $(dG\text{-}dC)_{15}$, it has been observed that the orientation of C-TPT form in the minor groove is in such a way that 10-OH and 9-dimethyl amino methylene groups are projecting outward from the groove, and therefore, it can access water environment, which is essential for the excited state conversion to Z^* form by ESPT process. In case of natural DNA, orientation of C-TPT is found to be similar as that of $(dG\text{-}dC)_{15}$. However, it is found that in case of $(dA\text{-}dT)_{15}$ bound C-TPT conformer, there are some conformer where -OH group is projecting inside the minor groove, and it cannot access water. As a result, ESPT process, which leads to the conversion of C to Z^* in the excited state, does not take place. Hence, we have observed a slight emission from C^* along with Z^* in case of $(dA\text{-}dT)_{15}$.

Acknowledgments

This work is partly supported by SERC, the Department of Science and Technology (DST), and Council of Scientific and Industrial Research (CSIR), Government of India. HJ thanks DST for the fellowship. AS is thankful to CSIR for providing CSIR-SRF fellowship. Authors thank to the Director, IISER-Pune for providing excellent experimental and computation facilities. Authors thank the reviewers for their constructive comments and suggestions.

View Article Online
DOI: 10.1039/C3RA42462F

Reference

1. B. D. Bax, P. F. Chan, D. S. Eggleston, A. Fosberry, D. R. Gentry, F. Gorrec, I. Giordano, M. M. Hann, A. Hennessy, M. Hibbs, J. Huang, E. Jones, J. Jones, K. K. Brown, C. J. Lewis, E. W. May, M. R. Saunders, O. Singh, C. E. Spitzfaden, C. Shen, A. Shillings, A. J. Theobald, A. Wohlkonig, N. D. Pearson and M. N. Gwynn, *Nature*, 2010, **466**, 935-940.

2. C.-C. Wu, T.-K. Li, L. Farh, L.-Y. Lin, T.-S. Lin, Y.-J. Yu, T.-J. Yen, C.-W. Chiang and N.-L. Chan, *Science*, 2011, **333**, 459-462.

3. K. Garber, *Nature*, 2012, **489**, S4-S6.

4. L. F. Liu, P. Duann, C.-T. Lin, P. D'Arpa and J. Wu, *Ann. N.Y. Acad. Sci.*, 1996, **803**, 44-49.

5. M. E. Wall, M. C. Wani, C. E. Cook, K. H. Palmer, A. T. McPhail and G. A. Sim, *J. Am. Chem. Soc.*, 1966, **88**, 3888-3890.

6. L. B. Grochow, E. K. Rowinsky, R. Johnson, S. Ludeman, S. H. Kaufmann, F. L. McCabe, B. R. Smith, L. Hurowitz, A. DeLisa and R. C. Donehower, *Drug Metab. Dispos.*, 1992, **20**, 706-713.

7. L. P. Rivory and J. Robert, *Pharmacol. Therapeut.*, 1995, **68**, 269-296.

8. Y.-H. Hsiang, M. G. Lihou and L. F. Liu, *Cancer Res.*, 1989, **49**, 5077-5082.

9. Y. H. Hsiang, R. Hertzberg, S. Hecht and L. F. Liu, *J. Biol. Chem.*, 1985, **260**, 14873-14878.

10. M. L. Rothenberg, *Ann. Oncol.*, 1997, **8**, 837-855.

11. B. L. Staker, K. Hjerrild, M. D. Feese, C. A. Behnke, A. B. Burgin and L. Stewart, *Proc. Natl. Acad. Sci. U.S.A.*, 2002, **99**, 15387-15392.

12. S. Yao, D. Murali, P. Seetharamulu, K. Haridas, P. N. V. Petluru, D. G. Reddy and F. H. Hausheer, *Cancer Res.*, 1998, **58**, 3782-3786.

13. M. R. di Nunzio, Y. Wang and A. Douhal, *J. Phys. Chem. B*, 2012, **116**, 7522-7530.

14. M. R. di Nunzio, Y. Wang and A. Douhal, *J. Phys. Chem. B*, 2012, **116**, 8182-8190.

15. K. Gavvala, A. Sengupta, R. K. Koninti and P. Hazra, *ChemPhysChem*, 2013, **14**, 3375-3383.

16. J. Fassberg and V. J. Stella, *J. Pharm. Sci.*, 1992, **81**, 676-684.

View Article Online
DOI: 10.1039/C3RA42462F

17. P. Tardi, E. Choice, D. Masin, T. Redelmeier, M. Bally and T. D. Madden, *Cancer Res.*, 2000, **60**, 3389-3393.

18. J. Du, W.-L. Lu, X. Ying, Y. Liu, P. Du, W. Tian, Y. Men, J. Guo, Y. Zhang, R.-J. Li, J. Zhou, J.-N. Lou, J.-C. Wang, X. Zhang and Q. Zhang, *Mol. Pharm.*, 2009, **6**, 905-917.

19. C. Foulon, J. Tedou, T. Queruau Lamerie, C. Vaccher, J. P. Bonte and J. F. Goossens, *Tetrahedron: Asymmetry*, 2009, **20**, 2482-2489.

20. D. Yang, J. T. Strode, H. P. Spielmann, A. H. J. Wang and T. G. Burke, *J. Am. Chem. Soc.*, 1998, **120**, 2979-2980.

21. J. Feigon, W. A. Denny, W. Leupin and D. R. Kearns, *J. Med. Chem.*, 1984, **27**, 450-465.

22. F. A. Tanious, J. M. Veal, H. Buczak, L. S. Ratmeyer and W. D. Wilson, *Biochemistry*, 1992, **31**, 3103-3112.

23. W. D. Wilson, F. A. Tanious, D. Ding, A. Kumar, D. W. Boykin, P. Colson, C. Houssier and C. Bailly, *J. Am. Chem. Soc.*, 1998, **120**, 10310-10321.

24. S. Streltsov, A. Sukhanova, A. Mikheikin, S. Grokhovsky, A. Zhuze, I. Kudelina, K. Mochalov, V. Oleinikov, J.-C. Jardillier and I. Nabiev, *J. Phys. Chem. B*, 2001, **105**, 9643-9652.

25. F. Zunino, F. Animati and G. Capranico, *Curr. Pharm. Design*, 1995, **1**, 83-94.

26. J. B. Gibbs, *Science*, 2000, **287**, 1969-1973.

27. G. Manolov, Y. Manolova, A. Levan and G. Klein, *Hereditas*, 1971, **68**, 235-244.

28. B. Weisblum and P. L. De Haseth, *Proc. Natl. Acad. Sci. U.S.A.*, 1972, **69**, 629-632.

29. E. Schröck, S. d. Manoir, T. Veldman, B. Schoell, J. Wienberg, M. A. Ferguson-Smith, Y. Ning, D. H. Ledbetter, I. Bar-Am, D. Soenksen, Y. Garini and T. Ried, *Science*, 1996, **273**, 494-497.

30. W. Powell, G. C. Machray and J. Provan, *Trends Plant Sci.*, 1996, **1**, 215-222.

31. A. van Belkum, S. Scherer, L. van Alphen and H. Verbrugh, *Microbiol. Mol. Biol. Rev.*, 1998, **62**, 275-293.

32. M. E. Reichmann, S. A. Rice, C. A. Thomas and P. Doty, *J. Am. Chem. Soc.*, 1954, **76**, 3047-3053.

33. A. Sengupta and P. Hazra, *Chem. Phy. Lett.*, 2010, **501**, 33-38.

View Article Online
DOI: 10.1039/C3RA42462F

34. A. Sengupta, W. D. Sasikala, A. Mukherjee and P. Hazra, *ChemPhysChem*, 2012, **13**, 2142-2153.

35. K. Gavvala, W. D. Sasikala, A. Sengupta, S. A. Dalvi, A. Mukherjee and P. Hazra, *Phys. Chem. Chem. Phys.*, 2013, **15**, 330-340.

36. Krishna Gavvala, Abhigyan Sengupta and P. Hazra, *ChemPhysChem*, 2013.

37. T. Moreno, J. Pous, J. A. Subirana and J. L. Campos, *Acta Crystallogr. D*, 2010, **66**, 251-257.

38. Youri Timsit and D. Moras, *EMBO J.*, 1994, **13**, 2737-2746.

39. B. F. Eichman, J. M. Vargason, B. H. M. Mooers and P. S. Ho, *Proc. Natl. Acad. Sci. U.S.A.*, 2000, **97**, 3971-3976.

40. P. A. Holt, J. B. Chaires and J. O. Trent, *J. Chem. Inf. Model.*, 2008, **48**, 1602-1615.

41. G. M. Morris, D. S. Goodsell, R. S. Halliday, R. Huey, W. E. Hart, R. K. Belew and A. J. Olson, *J. Comput. Chem.*, 1998, **19**, 1639-1662.

42. G. M. Morris, R. Huey, W. Lindstrom, M. F. Sanner, R. K. Belew, D. S. Goodsell and A. J. Olson, *J. Comput. Chem.*, 2009, **30**, 2785-2791.

43. E. F. Pettersen, T. D. Goddard, C. C. Huang, G. S. Couch, D. M. Greenblatt, E. C. Meng and T. E. Ferrin, *J. Comput. Chem.*, 2004, **25**, 1605-1612.

44. R. M. Izatt, J. J. Christensen and J. H. Rytting, *Chem. Rev.*, 1971, **71**, 439-481.

45. A. Sen and M. Maiti, *Biochem. Pharmacol.*, 1994, **48**, 2097-2102.

46. C. V. Kumar and E. H. Asuncion, *J. Am. Chem. Soc.*, 1993, **115**, 8547-8553.

47. K. M. Solntsev, E. N. Sullivan, L. M. Tolbert, S. Ashkenazi, P. Leiderman and D. Huppert, *J. Am. Chem. Soc.*, 2004, **126**, 12701-12708.

48. C. Eggeling, J. R. Fries, L. Brand, R. Günther and C. A. M. Seidel, *Proc. Natl. Acad. Sci. U.S.A.*, 1998, **95**, 1556-1561.

49. D. Řeha, M. Kabeláč, F. Ryjáček, J. Šponer, J. E. Šponer, M. Elstner, S. Suhai and P. Hobza, *J. Am. Chem. Soc.*, 2002, **124**, 3366-3376.

50. T. Heinlein, J.-P. Knemeyer, O. Piestert and M. Sauer, *J. Phys. Chem. B*, 2003, **107**, 7957-7964.

51. Y. Sun, F. Ji, R. Liu, J. Lin, Q. Xu and C. Gao, *J. Lumin.*, 2012, **132**, 507-512.

View Article Online
DOI: 10.1039/C3RA42462F

52. D. Sahoo, P. Bhattacharya and S. Chakravorti, *J. Phys. Chem. B*, 2010, **114**, 2044-2050.

53. Y. Shi, C. Guo, Y. Sun, Z. Liu, F. Xu, Y. Zhang, Z. Wen and Z. Li, *Biomacromolecules*, 2011, **12**, 797-803.

54. B. K. Paul and N. Guchhait, *J. Phys. Chem. B*, 2011, **115**, 11938-11949.

55. F. M. Pohl, T. M. Jovin, W. Baehr and J. J. Holbrook, *Proc. Natl. Acad. Sci. U.S.A.*, 1972, **69**, 3805-3809.

56. Q. Guo, M. Lu, L. A. Marky and N. R. Kallenbach, *Biochemistry*, 1992, **31**, 2451-2455.

57. Udo Heinemann, Cladudia Alings and M. Bansal, *EMBO J.*, 1992, **11**, 1931-1939.

58. H. C. M. Nelson, J. T. Finch, B. F. Luisi and A. Klug, *Nature*, 1987, **330**, 221-226.

59. I. D. Vladescu, M. J. McCauley, I. Rouzina and M. C. Williams, *Phys. Rev. Lett.*, 2005, **95**, 158102.

60. F. Zsila, Z. Bikadi and M. Simonyi, *Org. Biomol. Chem.*, 2004, **2**, 2902-2910.

61. M. Egli, *Chem. Biol.*, 2002, **9**, 277-286.

62. N. V. Hud and M. Polak, *Curr. Opin. Struc. Biol.*, 2001, **11**, 293-301.

63. A. Rodger and B. Nordén, *Circular Dichroism & Linear Dichroism*, Oxford University Press Inc., New York, United States, 1997.

64. Victor A Bloomfield, Donald M Crothers and I. Tinoco, *Nucleic Acids: Structures, Properties and Functions*, University Science Books, Sausalito, 2000.

65. J. Kypr, I. Kejnovská, D. Renčiuk and M. Vorlíčková, *Nucleic Acids Res.*, 2009, **37**, 1713-1725.

66. D. Sarkar, P. Das, S. Basak and N. Chattopadhyay, *J. Phys. Chem. B*, 2008, **112**, 9243-9249.

67. J. R. Lakowicz, *Principles of Fluorescence Spectroscopy*, Third Edition edn., Springer, 2006.

68. F. G. R., *Chemical applications of ultrafast spectroscopy*, Oxford university press, New York, 1986.

View Article Online
DOI: 10.1039/C3RA42462F

Table 1a. Time-resolved fluorescence decay parameters of TPT in absence and presence of dsDNAs collected at 530 nm.

Sample	τ_1	τ_2	a_1	a_2	τ_{av}[b]	χ^2
TPT in PB pH 5.1	0.79	5.79	0.07	0.93	5.43	1.01
$(dG\text{-}dC)_{15}$ 10 μM	0.69	5.80	0.07	0.93	5.42	1.07
$(dG\text{-}dC)_{15}$ 100 μM	1.26	5.80	0.05	0.95	5.59	1.11
$(dA\text{-}dT)_{15}$ 10 μM	1.61	6.01	0.12	0.88	5.46	1.04
$(dA\text{-}dT)_{15}$ 100 μM	2.28	6.60	0.26	0.74	5.49	1.14
CT-DNA 10 μM	1.7	5.80	0.05	0.95	5.6	1.21
CT-DNA 100 μM	1.09	5.80	0.07	0.93	5.45	0.97

[b] $\tau_{av} = (\tau_1 a_1 + \tau_2 a_2)$

Table 1b. Time-resolved fluorescence decay parameters of TPT in absence and presence of dsDNAs collected at 420 nm.

Sample	τ_1	τ_2	τ_3	a_1	a_2	a_3	τ_{av}[b]	χ^2
$(dA\text{-}dT)_{15}$ 10 μM	0.06	0.42	1.7	0.61	0.32	0.07	0.30	1.3
$(dA\text{-}dT)_{15}$ 40 μM	0.08	0.50	2.1	0.5	0.42	0.08	0.42	1.2
$(dA\text{-}dT)_{15}$ 100 μM	0.08	0.47	1.9	0.45	0.44	0.10	0.45	1.3

[b] $\tau_{av} = (\tau_1 a_1 + \tau_2 a_2 + \tau_3 a_3)$

View Article Online
DOI: 10.1039/C3RA42462F

Table 2. Anisotropy decay parameters of TPT in absence and presence of dsDNAs (λ_{ex} = 375 nm).

Sample	τ_{1r}	τ_{2r}	a_{1r}	a_{2r}	χ^2
TPT in PB pH 5.1, (λ_{em} = 530 nm)	0.24	-	1	-	1.02
$(dG\text{-}dC)_{15}$ 100 μM, (λ_{em} = 530 nm)	0.23	-	1	-	1.02
$(dA\text{-}dT)_{15}$ 100 μM, (λ_{em} = 530 nm)	4.28	0.32	0.46	0.54	1.07
CT-DNA 100 μM, (λ_{em} = 530 nm)	0.24	-	1	-	1.04
$(dA\text{-}dT)_{15}$ 100 μM, (λ_{em} = 420 nm)	1.70	0.08	0.60	0.40	1.2

View Article Online
DOI: 10.1039/C3RA42462F

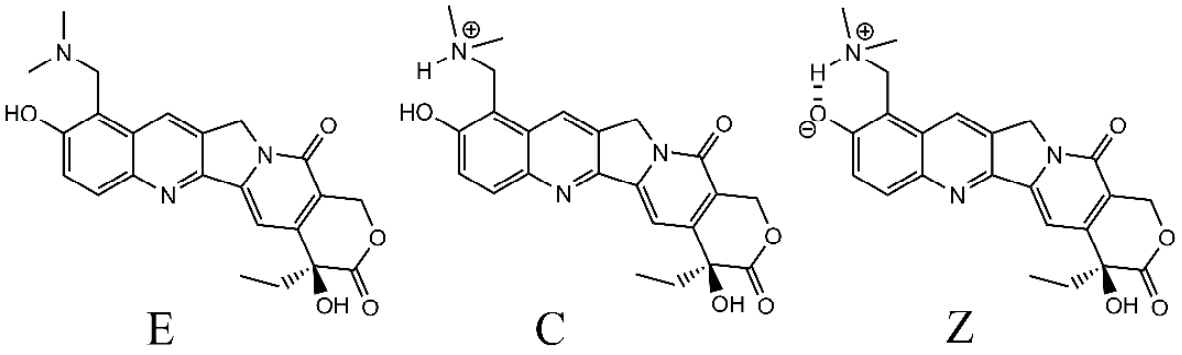

Scheme 1. Different prototropic forms of TPT in aqueous solution.

View Article Online
DOI: 10.1039/C3RA42462F

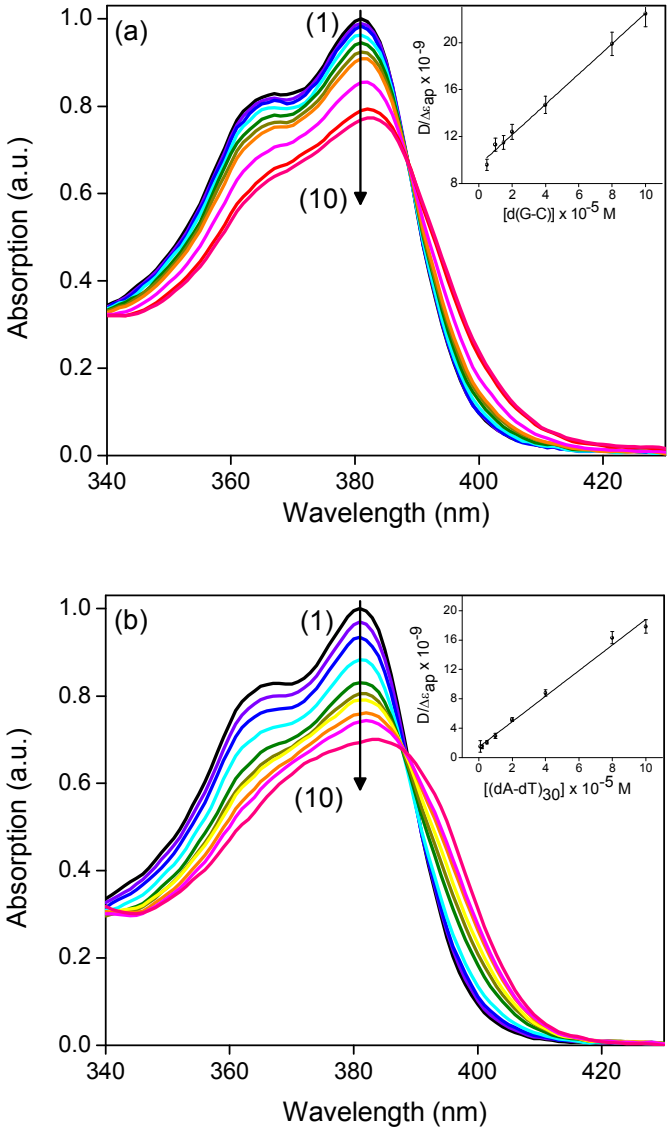

Figure 1. Absorption spectra of TPT (20 μM) in presence of (a) $(dG\text{-}dC)_{15}$ and (b) $(dA\text{-}dT)_{15}$. 1→10 represents DNA concentrations 0, 1, 2, 5, 10, 15, 20, 40, 80, and 100 μM, respectively. Inset shows the half reciprocal plot used to calculate binding constants.

View Article Online
DOI: 10.1039/C3RA42462F

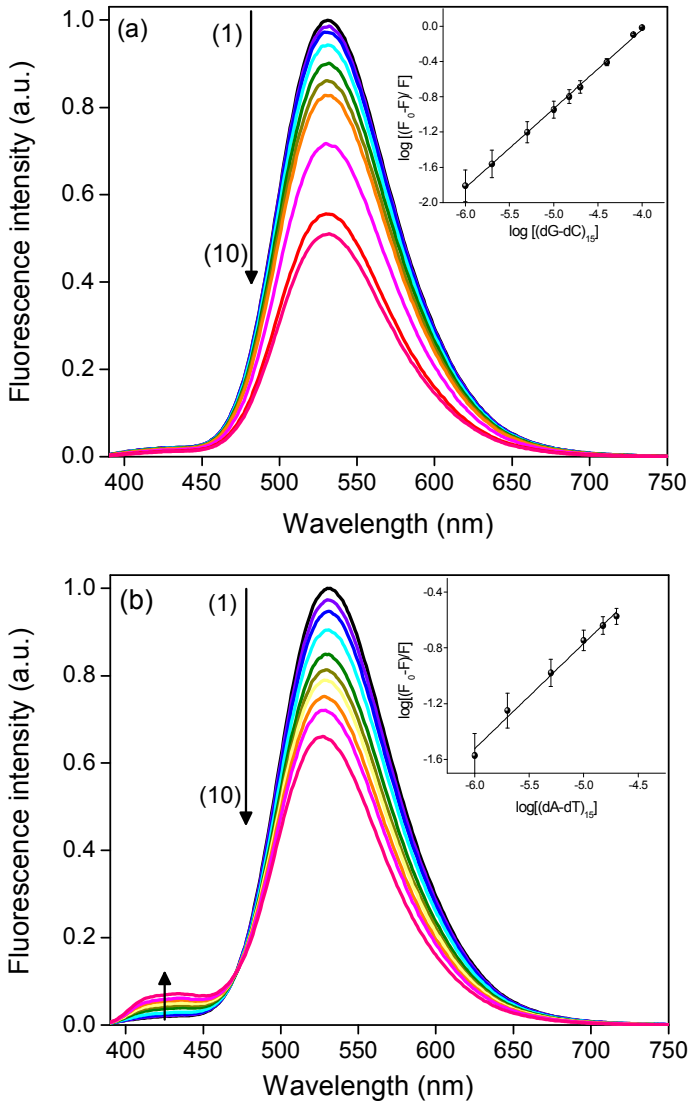

Figure 2. Fluorescence emission spectra of TPT (20 μM) in presence of (a) $(dG\text{-}dC)_{15}$ and (b) $(dA\text{-}dT)_{15}$. 1→10 represents DNA concentrations 0, 1, 2, 5, 10, 15, 20, 40, 80 and 100 μM, respectively. Inset shows double logarithmic plot for the determination of binding constant.

View Article Online
DOI: 10.1039/C3RA42462F

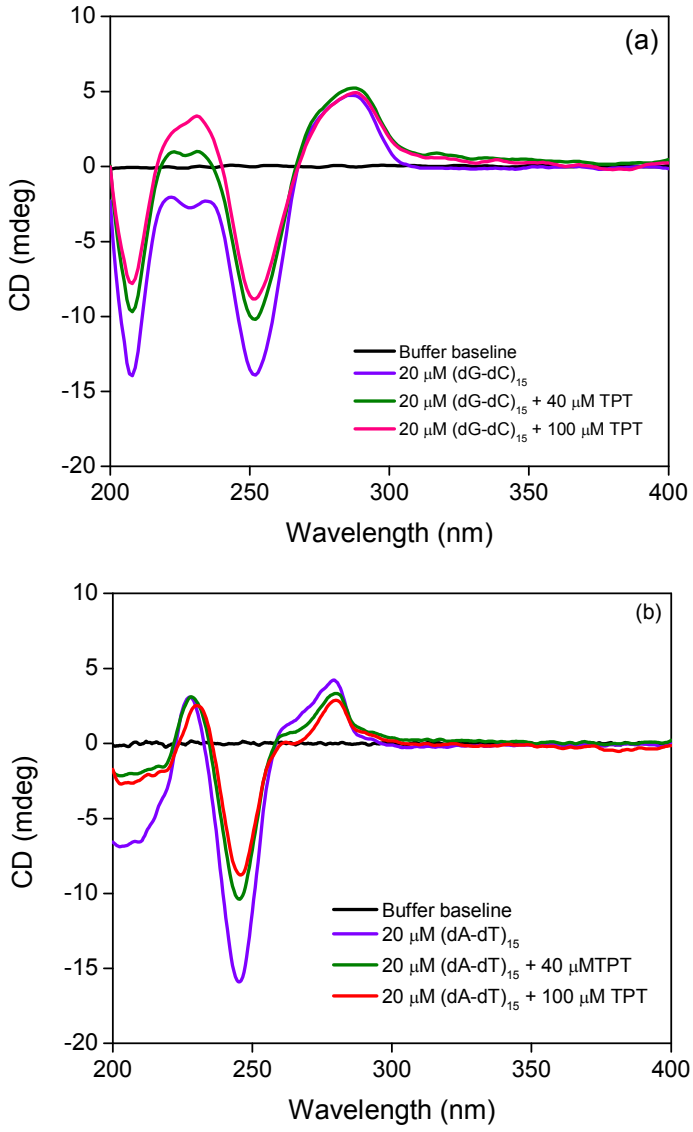

Figure 3. CD spectral profiles of (a) $(dG\text{-}dC)_{15}$ and (b) $(dA\text{-}dT)_{15}$ in presence of varying concentrations of TPT.

View Article Online
DOI: 10.1039/C3RA42462F

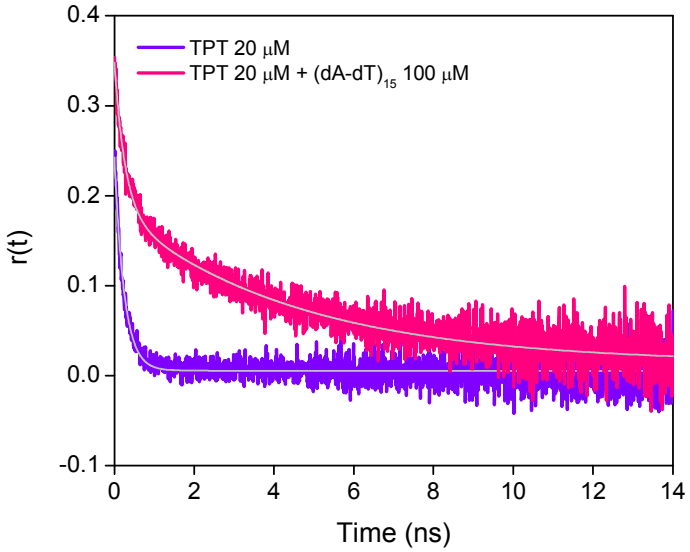

Figure 4. Time-resolved fluorescence anisotropy decay profile of TPT in buffer (pH 5.1) and in presence of $(dA\text{-}dT)_{15}$. λ_{ex}= 375 nm, $\lambda_{Collection}$ = 530 nm.

View Article Online
DOI: 10.1039/C3RA42462F

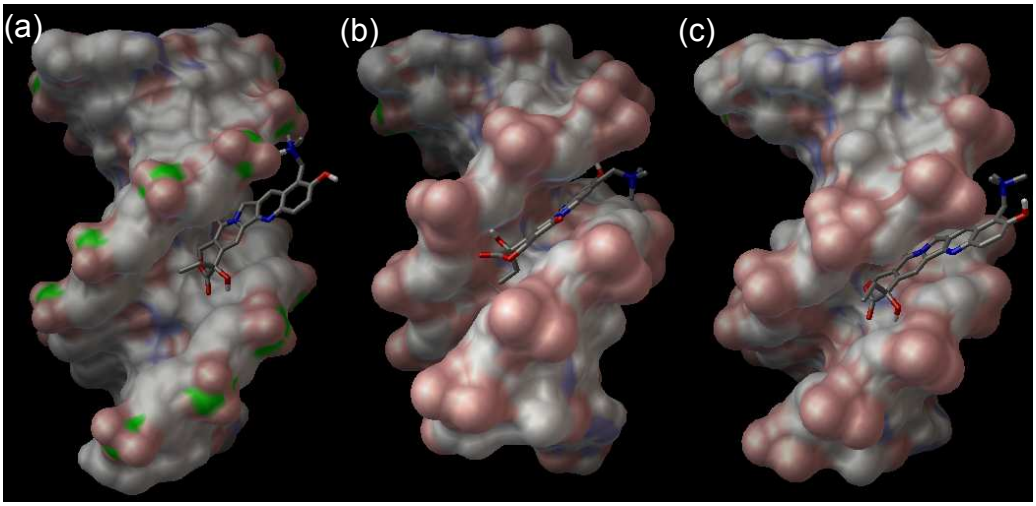

Figure 5. Docking structures of C-TPT when bind with (a) poly(dG-dC) and (b), (c) poly(dA-dT).